Convection-diffusion Model For Alumina Concentration in Hall-Héroult Process

Lucas José da Silva Moreira, Gildas Besancon, Francesco Ferrante, Mirko Fiacchini, Hervé Roustan

Convection-diffusion Model For Alumina Concentration in Hall-Héroult Process ⋆

Lucas José da Silva Moreira * **Gildas Besançon** *
Francesco Ferrante ** **Mirko Fiacchini** * **Hervé Roustan** ***

* *Univ. Grenoble Alpes, CNRS, Grenoble INP, GIPSA-lab, Grenoble, France. (e-mail: lucas-jose.da-silva-moreira, mirko.fiacchini , gildas.besancon @grenoble-inp.fr).*
** *Department of Engineering, University of Perugia, Via G. Duranti, 67, 06125 Perugia, Italy, (email: francesco.ferrante@unipg.it)*
*** *Rio Tinto, Laboratoire de Recherche des Fabrications, Saint Jean de Maurienne, France(e-mail: herve.roustan@riotinto.com)*

Abstract: Hall-Héroult process is an electrolysis method to produce aluminum at industrial scale. It is based on an electrochemical reaction that requires an alumina dissolution in a bath solution. The hazardous operational conditions make it difficult the development of a sensor for continuous measurement. Moreover, local variations of alumina concentration throughout the pot cell arise during daily operations. This paper presents a modeling procedure to obtain a spatio-temporal dynamic representation of alumina concentration distribution. From the convection-diffusion relations, the alumina source term is analyzed and expanded to obtain the relations between the available signals and the output. The goal is to develop a system that is able to predict the obtained measurement by taking into account transport properties. The model is validated with industrial data and compared with other models.

Keywords: Hall-Héroult process, Process Modeling

1. INTRODUCTION

The Hall-Héroult process is the main industrial procedure to obtain pure aluminum (Grjotheim and Welch, 1980). It consists in an electrolysis reaction that is able to isolate the aluminum element from alumina (Al_2O_3). It first requires to dip carbon anodes into a high temperature liquid bath solution. Then, a high intensity electric current is applied to the cell, making the liquid aluminum to accumulate at the bottom. Besides it, carbon dioxide is released during the electrolysis procedure. A schematic pot cell is shown in Figure 1 and the main chemical reaction that summarizes the process is:

$$Al_2O_{3(diss)} + \frac{3}{2}C_{(anode)} \rightarrow 2Al_{(l)} + \frac{3}{2}CO_{2(g)} \qquad (1)$$

Usually, the pot cells operate with extreme conditions as high temperature and magnetic field. Moreover, the bath solution has corrosive elements. Hence, continuous measurements possibilities are limited during cell operation. The process production efficiency is constrained and experimental models are inaccurate due the lack of data (Jakobsen et al., 2001).

One of the essential states for regulation is the alumina concentration (wAl_2O_3). It is desired to have this element in a certain range. If there is a low concentration, it could trigger an *anode effect*, a deleterious phenomenon leading to the production of greenhouse gases (Bearne, 1999). On the other hand, a large concentration could create a sludge phenomenon, an accumulation of undissolved alumina and bath at the bottom of the cell. In this case, the dissolution is slower than usual and it is erosive to the cathode which can lead damage the cell (Biedler, 2003). Commonly, just a few measurements of the alumina concentration per week are manually taken, which makes it difficult to obtain an experimental model.

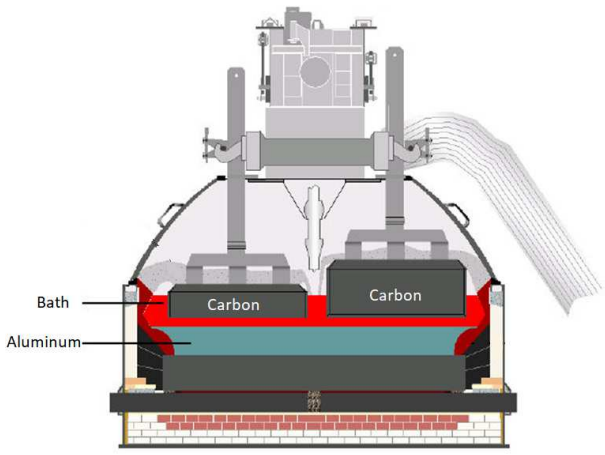

Fig. 1. Pot Schematic View

Some researches have been developing models to estimate the alumina concentration distribution according to observers design (Yao et al., 2017; Jakobsen et al., 2001). A

⋆ This research was partially supported by project "FUI-AAP 25 PIANO".

simulator that computes the alumina concentration distribution was developed by Dion et al. (2018) to predict anode effects. In da Silva Moreira et al. (2020a,b), the alumina concentration is estimated for average conditions from an experimental model.

This paper presents a model that captures the main alumina concentration distribution dynamics, allowing to predict the next collected sample. From each individual feeding signal, convection-diffusion equation and process parameters, it is possible to compute the alumina concentration distribution. This procedure is validated with operational collected data and tested for different conditions in APX pot cell of Rio Tinto Laboratoire des Recherches de Fabrications (LRF) located in Saint Jean de Maurienne, France. For confidentiality reasons, the data in the y-axis in all plots have been avoided and the input signals are normalized by the initial value.

The paper is organized as follows: section 2 gives an overview of the problem description, section 3 presents the proposed modeling approach, and section 4 provides the validation procedure. Some conclusions are summarized in section 5.

2. PROCESS DESCRIPTION

Usually, the alumina is injected in powder condition through many feeders placed along the cell. They are operated by the same frequency signal (F) and have a specified selection order. The same amount of alumina is injected by each feeder once it is ordered. This feeding frequency, adjusted in function of the pseudo-resistance evolution, usually oscillates between overfeeding and underfeeding in order to keep the alumina concentration in the desired range. The regulation goal is to operate close to the optimal range, between 2% and 4% shown in Figure 2 (Haupin, 2016). However, the pot resistance value is also function of the anode-cathode distance (ACD) as well. Therefore, this regulation could be inaccurate since ACD and alumina concentration are not measured.

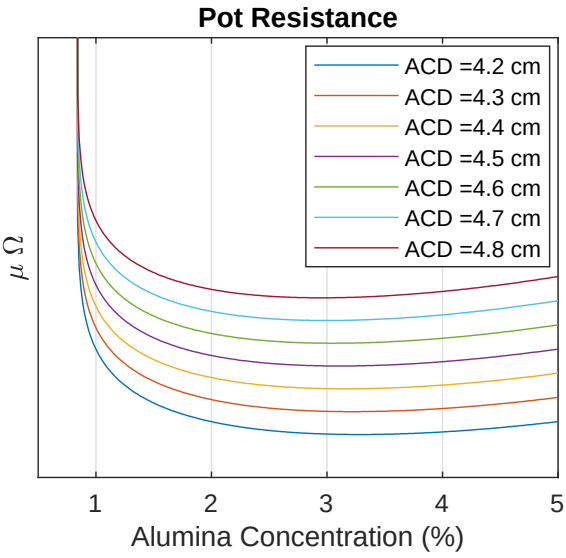

Fig. 2. Typical pot resistance curve as a function of alumina concentration and ACD

Furthermore, the pseudo-resistance value reflects a global state of the pot cell, however, the local conditions are not uniform. Each anode has its own electric current dynamics according to its operational age (Guérard and Côté, 2019). Hence, the current distribution is diverse and, then, the aluminum production rate varies accordingly along the cell and, the alumina consumption rate is different for each anode. The magnetic field distribution affects the bath fluid velocity and all transport elements in the solution. Moreover, the alumina is not instantly dissolved in the bath. Those conditions give rise to different alumina concentration values along the cell. Hence, it is important to obtain a model that is able to handle those conditions in order to enhance the production since the regulation is performed by global indicator and the process is non uniform.

In the pot cell used in this paper, the position grid is defined for the coordinates:

$$(x, y) \in \Omega \tag{2}$$

where Ω is the grid surface. Moreover, there are n_f feeders placed in fixed positions (x_f, y_f).

$$\begin{aligned}(x_f, y_f) &\in \{(x_1, y_1), (x_2, y_2), \cdots, (x_{n_f}, y_{n_f})\} \\ &= S_f\end{aligned} \tag{3}$$

They follow a predefined sequence to inject alumina in the pot, according to a frequency specified by the regulation. Moreover, the alumina sample is collected 3 times a day always around the same position to evaluate the process regulation. This sample will be used to compare the model precision. Furthermore, it is considered that the anodes have the same width and depth. In addition, the pot has the dimensions $x_{max} \times y_{max}$.

3. MODELING

The model we propose is based on the convection-diffusion equation (Kou, 1996). Moreover, the fluid transport relations in the solution are analyzed. Initially, the alumina concentration is defined by the ratio of the dissolved alumina mass in the bath and the total amount of bath mass in an infinitesimal region:

$$wAl_2O_3 = \frac{m_{Al_2O_3}}{m_{bath}} \tag{4}$$

where $m_{Al_2O_3}$ is the alumina mass dissolved in the bath and m_{bath} is the amount of mass in the bath. This relation is used in the following subsections.

3.1 Convection-Diffusion Equation

To obtain the dissolved alumina mass distribution model, it is necessary first to analyze the convection-diffusion equation (Kou, 1996) with $x \in [0, x_{max}]$ and $y \in [0, y_{max}]$. The equation is defined as:

$$\frac{\partial}{\partial t}c(t) = \nabla \cdot (D_e \nabla c(t)) - \nabla \cdot (\mathbf{u}c(t)) + R(t) \tag{5}$$

where c is the number of moles of alumina per volume in the solution that varies in space and time and, D_e a constant diffusion coefficient, $\mathbf{u}$ the flow velocity vector that varies only in space and R the sources of c that varies

in space and time. In order to simplify the notation, the space dependencies of the respective variables are hidden.

The source term R is defined by the sum of three components as:

$$R(t) = \overbrace{c_F(t)}^{\text{Input}} + \overbrace{c_S(t)}^{\text{Generation}} - \underbrace{c_C(t)}_{\text{Consumption}} \tag{6}$$

where all components vary in space and time. Moreover, a sampling time of 1 minute is chosen. According to Biedler (2003), the alumina dissolving dynamics can be split in fast and slow dissolution rates. Then, the fast alumina dissolving dynamics can be considered as an input source since the time constant is $0.099s^{-1}$. The generation term represents the slow dissolving dynamics. Each source term is described in the next subsections.

Input Source: The quantity injected in the pot by the feeders is the input term in equation (6):

$$c_F(t) = r\frac{m_{in}\rho_{bath}}{m_{bath}M_{Al_2O_3}}F_i(t) \tag{7}$$

where m_{in} is the mass amount injected, ρ_{bath} is the bath density, m_{bath} is the bath solution mass, $M_{Al_2O_3}$ is the alumina molecular mass, r is the weight ratio between the fast and slow dissolving alumina and $F_i(t)$ is the individual frequency of the feeder signal. This is an activation signal with same frequency as the global feeding according to a predefined order:

$$F_i(t) = sel_i(t)F(t) \tag{8}$$

where $sel_i(t)$ is a binary selection variable. By replacing equation (8) in (7):

$$c_F(t) = sel_i(t)r\frac{m_{in}\rho_{bath}}{m_{bath}M_{Al_2O_3}}F(t) \tag{9}$$

As the feeders are arranged in fixed positions on the pot S_f, this source is added as a limit conditions in each feeder position. Therefore:

$$c_F(t) = \begin{cases} sel_i(t)r\dfrac{m_{in}\rho_{bath}}{m_{bath}M_{Al_2O_3}}F(t) & \forall(x,y) \in S_f \\ 0 & \forall(x,y) \notin S_f \end{cases} \tag{10}$$

for $i = 1$ to n_f.

Generation Source: The generation term is function of the alumina dissolving rate in the bath solution. The slow dissolution can be approximated by the following equation equation:

$$c_S(t) = k_{diss}c_{un}(t) \tag{11}$$

where k_{diss} is the respective dissolution rate constant and c_{un} is the undissolved quantity. The dissolving dynamics is given by:

$$\frac{\partial}{\partial t}c_{un}(t) = \begin{cases} sel_i(t)(1-r)\dfrac{m_{in}\rho_{bath}}{m_{bath}(t)M_{Al_2O_3}}F(t) - k_{diss}c_{un}(t) & \forall(x,y) \in S_f \\ -k_{diss}c_{un}(t) & \forall(x,y) \notin S_f \end{cases} \tag{12}$$

for $i = 1$ to n_f.

Consumption Source: The consumption rate in an electrolysis reaction is given by Faraday's law and chemical balance. In order to produce 1 mol of Al it is required to consume $1/2$ moles of Al_2O_3 according to equation (1). Then, the consumption source is given by:

$$c_C(t) = \frac{\rho_{bath}}{6\mathfrak{F}m_{bath}(t)}I(t) \tag{13}$$

where I is the electric current for an anode or the sum of a desired region and $\mathfrak{F}$ *is the Faraday's constant.*

3.2 Distribution Model

Based on (10), (11) and (13), the equation (5) can be used to investigate the fluid proprieties distribution in the solution. The bath flow velocity is time invariant and it is defined as:

$$\mathbf{u} = u_x(x,y)\widehat{i} + u_y(x,y)\widehat{j} \tag{14}$$

with u_x and u_y are known for all values of x and y, $\widehat{i}$ and $\widehat{j}$ are unity vectors in x and y directions respectively. The flow distribution inside the pot cell was given by Rio Tinto modeling team.

Moreover, assuming D_e as a constant, equation (5) becomes:

$$\frac{\partial}{\partial t}c(t) = D_e\nabla^2 c(t) - \nabla\cdot(\mathbf{u}c(t)) + R(t) \tag{15}$$

Furthermore, convection term $(\nabla\cdot(\mathbf{u}c))$ in equation (15) can be expanded as:

$$\frac{\partial}{\partial t}c(t) = D_e\nabla^2 c(t) - [c(t)(\nabla\cdot\mathbf{u}) + \mathbf{u}(\nabla\cdot c(t))] + R(t) \tag{16}$$

As the fluid is incompressible, it is assumed:

$$\nabla\cdot\mathbf{u} = 0 \tag{17}$$

Then, equation (16) can be simplified and it becomes:

$$\frac{\partial}{\partial t}c(t) = D_e\nabla^2 c(t) - \mathbf{u}(\nabla\cdot c(t)) + R(t) \tag{18}$$

By expanding equation (18):

$$\frac{\partial}{\partial t}c(t) = D_e\left(\frac{\partial^2}{\partial x^2}c(t) + \frac{\partial^2}{\partial y^2}c(t)\right) - \left(u_x(x,y)\frac{\partial}{\partial x}c(t) + u_y(x,y)\frac{\partial}{\partial y}c(t)\right) + R(t) \tag{19}$$

This equation represents the moles concentration in the distribution.

To obtain equation (19) as a function of the alumina concentration, it is necessary to express c in terms of wAl_2O_3. By definition, c is the number of alumina moles $n_{Al_2O_3}$ per bath volume V_{bath}:

$$c(t) = \frac{n_{Al_2O_3}(t)}{V_{bath}(t)} \tag{20}$$

The number of moles is the ratio between the element mass and molar mass ($n_{Al_2O_3}(t) = \frac{m_{Al_2O_3}(t)}{M_{Al_2O_3}}$) and the bath

volume is the ratio between mass and density ($V_{bath}(t) = \frac{m_{bath}(t)}{\rho_{bath}}$). Hence, equation (20) becomes:

$$c(t) = \frac{\frac{m_{Al_2O_3}(t)}{M_{Al_2O_3}}}{\frac{m_{bath}(t)}{\rho_{bath}}} \tag{21}$$

Organizing equation (21):

$$c(t) = \frac{1}{M_{Al_2O_3}} \rho_{bath} \left(\frac{m_{Al_2O_3}(t)}{m_{bath}(t)} \right) \tag{22}$$

Replacing equation (4) in (22):

$$c(t) = \frac{\rho_{bath}}{M_{Al_2O_3}} wAl_2O_3(t) \tag{23}$$

Giving the relation between wAl_2O_3 and c. Assuming ρ_{bath} as a constant, the equations (19) and (23) can be written as:

$$\begin{aligned} \frac{\rho_{bath}}{M_{Al_2O_3}} \frac{\partial}{\partial t} wAl_2O_3(t) = D_e \frac{\rho_{bath}}{M_{Al_2O_3}} \Bigg(& \frac{\partial^2}{\partial x^2} wAl_2O_3(t) \\ & + \frac{\partial^2}{\partial y^2} wAl_2O_3(t) \Bigg) \\ - \frac{\rho_{bath}}{M_{Al_2O_3}} \Bigg(& u_x(x,y) \frac{\partial}{\partial x} wAl_2O_3(t) \\ & + u_y(x,y) \frac{\partial}{\partial y} wAl_2O_3(t) \Bigg) + R(t) \end{aligned} \tag{24}$$

By simplifying the term $\frac{\rho_{bath}}{M_{Al_2O_3}}$, equation (24) can be written as:

$$\begin{aligned} \frac{\partial}{\partial t} wAl_2O_3(t) = D_e & \left(\frac{\partial^2}{\partial x^2} wAl_2O_3(t) + \frac{\partial^2}{\partial y^2} wAl_2O_3(t) \right) \\ & - \left(u_x \frac{\partial}{\partial x} wAl_2O_3(t) + u_y \frac{\partial}{\partial y} wAl_2O_3(t) \right) \\ & + \frac{M_{Al_2O_3}}{\rho_{bath}} R(t) \end{aligned} \tag{25}$$

Equation (25) represents spatio-temporal dynamics of the alumina concentration from the feeding and current distribution signals. The undissolved alumina concentration wAl_2O_{3un} model is obtained by replacing equation (23) in (12):

$$\begin{aligned} & \frac{\partial}{\partial t} wAl_2O_{3un}(t) \\ & = \begin{cases} sel_i(t)(1-r)\frac{m_{in}}{m_{bath}(t)} F(t) - \frac{M_{Al_2O_3}}{\rho_{bath}} k_{diss} wAl_2O_{3un}(t) & \forall \{x,y\} \in S_f \\ -\frac{M_{Al_2O_3}}{\rho_{bath}} k_{diss} wAl_2O_{3un}(t) & \forall \{x,y\} \notin S_f \end{cases} \end{aligned} \tag{26}$$

4. VALIDATION

Once the model is stated, it is necessary to define some conditions in order to simulate the partial differential equation (25). It can be assumed that initial condition is uniform in the pot:

$$wAl_2O_3(x,y,0) = C_0 \ \forall (x,y) \in \Omega \tag{27}$$

where C_0 is a the initial alumina concentration value and Ω is the grid surface. Furthermore, the initial undissolved concentration of alumina concentration is defined as zero along the pot as well:

$$wAl_2O_{3un}(x,y,0) = 0 \ \forall (x,y) \in \Omega \tag{28}$$

The boundary conditions are set as:

$$\begin{aligned} & wAl_2O_3(0,y,t) = C_0 \\ & wAl_2O_3(x,0,t) = C_0 \\ & wAl_2O_3(x_{max},y,t) = C_0 \\ & wAl_2O_3(x,y_{max},t) = C_0 \\ & \frac{\partial}{\partial x} wAl_2O_3(0,y,t) = 0 \\ & \frac{\partial}{\partial x} wAl_2O_3(x,0,t) = 0 \\ & \frac{\partial}{\partial x} wAl_2O_3(x_{max},y,t) = 0 \\ & \frac{\partial}{\partial x} wAl_2O_3(x,y_{max},t) = 0 \\ & \frac{\partial}{\partial y} wAl_2O_3(0,y,t) = 0 \\ & \frac{\partial}{\partial y} wAl_2O_3(x,0,t) = 0 \\ & \frac{\partial}{\partial y} wAl_2O_3(x_{max},y,t) = 0 \\ & \frac{\partial}{\partial y} wAl_2O_3(x,y_{max},t) = 0 \end{aligned} \tag{29}$$

$$\begin{aligned} & wAl_2O_{3un}(0,y,t) = 0 \\ & wAl_2O_{3un}(x,0,t) = 0 \\ & wAl_2O_{3un}(x_{max},y,t) = 0 \\ & wAl_2O_{3un}(x,y_{max},t) = 0 \end{aligned} \tag{30}$$

To perform the simulation, three different grid sizes were chosen to verify the model accuracy: 7×1, 7×2 and 12×2. The values are chosen to verify the influence of each feeder in a certain area. Moreover, the anode electric current is supposed to be measured for each anode but its distribution in each anode surface is unknown. Then, the grid size is limited to the anodes number.

Each model is simulated using the same parameters. The simulations are reproduced in two scenarios. The first one is for a regular operation condition and there is an oscillation in the line current and in the second case, there are a feeding absence and current disturbance as well. To validate the results, the concentration average in the region close to the measure is compared with each system outputs. *The numerical implementation was done using the explicit method for discretization.*

4.1 Grid 7 ×1

The grid size of 7x1 is used to compare our model with the model described in Yao et al. (2017). As these models have only one dimension, the information in y-axis is ignored.

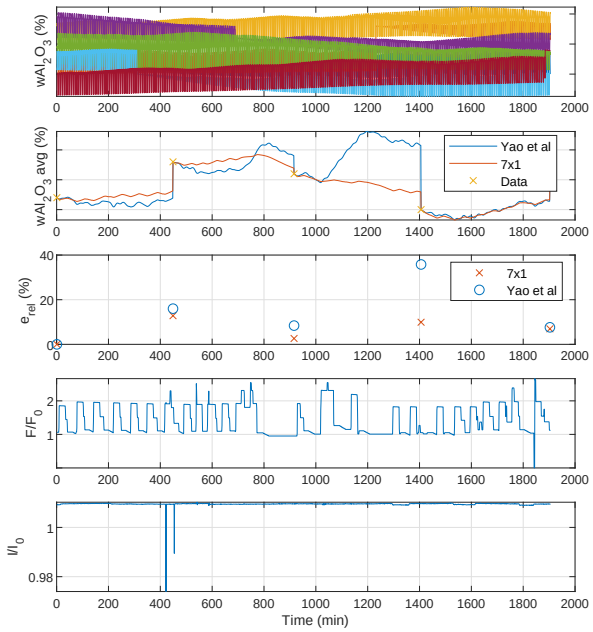

Fig. 3. Simulation Results - 7×1 grid - Scenario 1

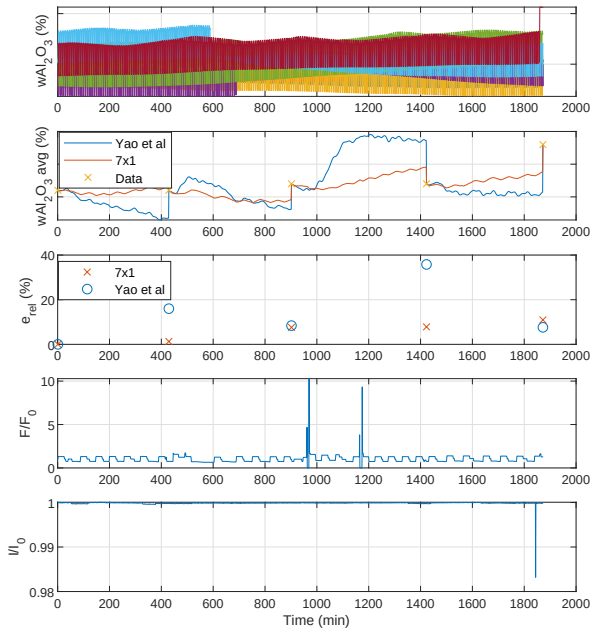

Fig. 4. Simulation Results - 7×1 grid - Scenario 2

Therefore, equation (25) is simplified into:

$$\frac{\partial}{\partial t}wAl_2O_3(t) = D_e\frac{\partial^2}{\partial x^2}wAl_2O_3(t) - u_x\frac{\partial}{\partial x}wAl_2O_3(t) + \frac{M_{Al_2O_3}}{\rho_{bath}}R(t) \tag{31}$$

Moreover, the currents are grouped for each area and the feeders are placed according to their position in the pot cell, this means that their values are added according to their position in the cell to fit in the grid size. Figure 3 shows alumina concentration evolution in time according to the feeding frequency and line current for each zone by a different color. *These are normalized from their respective initial values* F_0 and I_0. It can be seen that each line has an oscillation dynamics. Moreover, the collected data is displayed with the average concentration and the respective absolute relative error. According to the data, it can be noticed that the proposed model has a better fit with the measured data. All the errors are below 10%, except the value during the disturbance in the line current, around 400 min. Furthermore, their dynamics are similar. *Therefore, the proposed model can be used to accurately estimate the system.*

The same models are also tested for the second scenario in the presence of current disturbance and absence of feeding. The results are shown in Figure 4. It can be noticed that the proposed model has a better fit for all measurements. Therefore, this structure can simulate with a quite good accuracy the next measured sample.

4.2 Grid 7×2 and 12×2

The grid then is extended to take into account the dynamics in y-axis and the model is simulated for the same conditions, inputs and validation data previously used for two

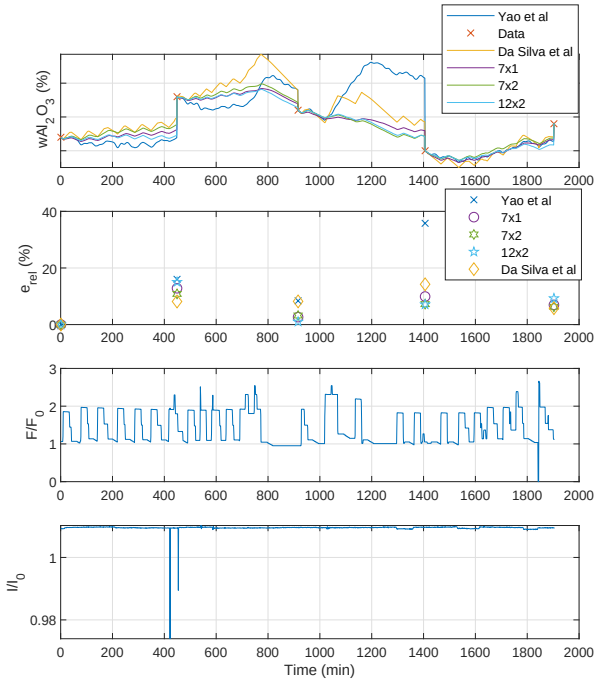

Fig. 5. Simulation Results - 7×2 and 12×2 grid - Scenario 1

different sizes: 7x2 and 12x2. The first one uses a structure similar to the previous size and the second one uses each current individually. In Figures 5 and 6, the results for the first and second scenario are shown respectively. Moreover, the model described in da Silva Moreira et al. (2020a,b) is also simulated and the results are displayed for accuracy comparison. Each mean absolute error is listed in Table 1.

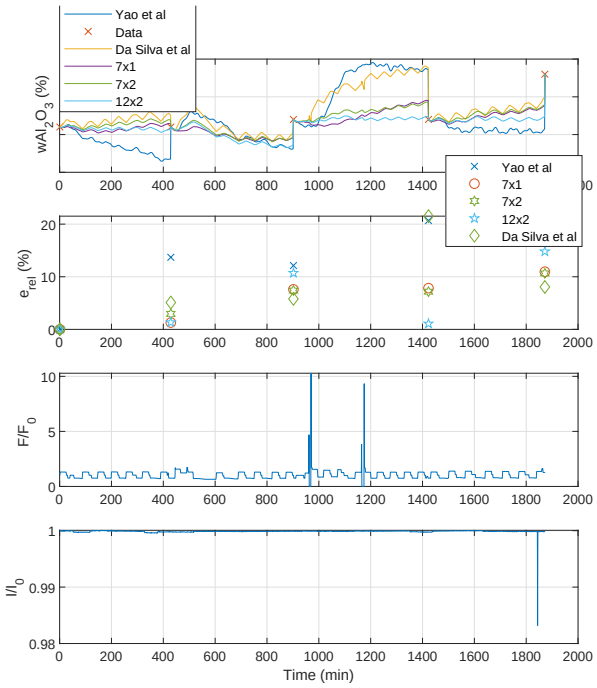

Fig. 6. Simulation Results - 7×2 and 12×2 grid - Scenario 2

Table 1. Mean absolute relative errors for alumina concentration models

	Scenario 1 (%)	Scenario 2 (%)
Yao et al.	16.95	16.40
7x1	8.08	6.92
7x2	6.88	7.03
12x2	8.10	6.98
Da Silva et al	9.09	10.11

From the results listed in Table 1, it can be noticed that the proposed models for any grid size have similar fits and they are smaller than in Yao et al. (2017) and da Silva Moreira et al. (2020a,b) results. Their accuracy is not affected by feeding absence or line current disturbance in general. This approach can thus be a good candidate for alumina concentration distribution prediction in a partial differential equation configuration.

5. CONCLUSIONS

This paper presented a model of the alumina concentration distribution. From the convection–diffusion equations, it was possible to develop a partial differential equation model that can allow to simulate the alumina dynamics along the pot cell. This system can be adjusted with different grid sizes and physical parameters.

By comparing the proposed system with other validated models, it was shown a good precision in the predictions. Moreover, it had some robustness against process input disturbances as well, since the prediction errors were small for these cases.

ACKNOWLEDGEMENTS

The authors wish to acknowledge project AAP 25 PIANO funded by the French Fonds Unique Interministériel (FUI).

REFERENCES

Bearne, G.P. (1999). The development of aluminum reduction cell process control. *JOM*, 51(5), 16–22.

Biedler, P. (2003). *Modeling of an aluminum reduction cell for the development of a state estimator*. Ph.D. thesis, West Virginia University.

da Silva Moreira, L.J., Besançon, G., Ferrante, F., Fiacchini, M., and Roustan, H. (2020a). Model based approach for online monitoring of aluminum production process. In *Light Metals 2020*, 566–571. Springer.

da Silva Moreira, L.J., Fiacchini, M., Besançon, G., Ferrante, F., and Roustan, H. (2020b). State affine modeling and observer design for Hall-Héroult process. In *IFAC World Congress 2020*.

Dion, L., Kiss, L.I., Poncsák, S., and Lagacé, C.L. (2018). Simulator of non-homogenous alumina and current distribution in an aluminum electrolysis cell to predict low-voltage anode effects. *Metallurgical and Materials Transactions B*, 49(2), 737–755.

Grjotheim, K. and Welch, B.J. (1980). *Aluminium Smelter Technology: A Pure and Applied Approach*. Aluminium-Verlag; 2nd edition.

Guérard, S. and Côté, P. (2019). A transient model of the anodic current distribution in an aluminum electrolysis cell. In *Light Metals 2019*, 595–603. Springer.

Haupin, W. (2016). Interpreting the components of cell voltage. In *Essential Readings in Light Metals*, 153–159. Springer.

Jakobsen, S.R., Hestetun, K., Hovd, M., and Solberg, I. (2001). Estimating alumina concentration distribution in aluminium electrolysis cells. *IFAC Proceedings Volumes*, 34(18), 303–308.

Kou, S. (1996). *Transport phenomena and materials processing*.

Yao, Y., Cheung, C.Y., Bao, J., Skyllas-Kazacos, M., Welch, B.J., and Akhmetov, S. (2017). Estimation of spatial alumina concentration in an aluminum reduction cell using a multilevel state observer. *AIChE Journal*, 63(7), 2806–2818.